

# Polishing of polycrystalline diamond by the technique of dynamic friction, part 1: Prediction of the interface temperature rise

Y. Chen<sup>a</sup>, L.C. Zhang<sup>a,\*</sup>, J.A. Arsecularatne<sup>a</sup>, C. Montross<sup>b</sup>

<sup>a</sup>*School of Aerospace, Mechanical and Mechatronic Engineering, The University of Sydney, Sydney NSW 2006, Australia*

<sup>b</sup>*Ringwood Superabrasives Pty. Ltd, 111 Gladstone St, Fyshwick ACT 2609, Australia*

Received 4 April 2005; accepted 7 July 2005

Available online 12 September 2005

## Abstract

This paper investigates the interface temperature rise in polishing a polycrystalline diamond (PCD) surface. First, the Greenwood–Williamson’s statistical asperity model is applied to characterise the surface roughness of a PCD specimen. The result is then used to estimate the contact area and total number of contact asperities under an applied polishing load. The heat generated is taken as the product of the friction force and the relative sliding velocity between the PCD asperities and the metal disk surface. The Jaeger’s moving heat source analysis is then applied to determine the fractions of heat flux flowing into the PCD asperities and their counterpart in contact sliding and to give rise to the average temperature rise. A comparison with the observations made in the authors’ experiments and those reported in the literature showed that the model predicts very well the temperature rise at the polishing interface.

© 2005 Elsevier Ltd. All rights reserved.

*Keywords:* Polycrystalline diamond (PCD); Temperature rise; Dynamic friction polishing

## 1. Introduction

Polycrystalline diamond (PCD) compacts are very attractive cutting tool materials because of their excellent properties such as ultra high hardness, thermal conductivity, strength, and chemical inertness to most corrosive environments. For precision machining applications, where PCD have been widely used, a cutting tool must have excellent surface finish and cutting edge sharpness. However, because of the ultra high hardness and chemical inertness of diamond, polishing of a PCD cutting tool is difficult. The traditional mechanical abrasive polishing technique has extremely low polishing rates, of the order of 10 nm/h, and therefore is time-consuming and costly [1]. Since 1988, various physical and chemical means have been explored to polish diamond and diamond films [2,3]. These include mechanical polishing [4, 5], chemically assisted mechanical polishing [6,7], thermochemical polishing [8–11], laser/plasma/ion beam polishing [2,12–14] and dynamic friction polishing [15,16], where

the dynamic friction method has been reported to be efficient and cost-effective. However, the control and optimization of the process have not been studied.

The dynamic friction polishing technique utilizes the thermochemical reaction between a diamond surface and a metal disk tool rotating at a high peripheral speed (Fig. 1). The polishing mechanisms can be described as: (a) conversion of diamond carbon into non-diamond carbon by friction heating and contacting with catalytic metals, which is then removed mechanically; (b) diffusion of carbon atoms into a counterpart metal and chemical reaction with the metal to form carbides; and (c) oxidization of carbon and evaporation in the form of CO or CO<sub>2</sub> gas. It is clear that chemical reaction of carbon plays an important role in the material removal of polishing PCD, with which carbon can react with metals or oxidate at an elevated temperature.

To control and then optimize the polishing of PCD using the friction dynamics mechanisms, the first step is to estimate the temperature rise during the process, find out the most effective ranges of polishing speed and pressure, and then establish their relation to the material removal rate. Hence, this very first paper of the authors’ series research will focus on the development of a model to predict the temperature rise of the PCD surface during polishing. Such

\* Corresponding author. Tel.: +61 2 9351 2835; fax: +61 2 9351 7060.  
E-mail address: [zhang@aeromech.usyd.edu.au](mailto:zhang@aeromech.usyd.edu.au) (L.C. Zhang).

## Nomenclature

|       |                                 |           |   |
|-------|---------------------------------|-----------|---|
| $A'$  | nominal area of PCD specimen    | $r$       | radius of polishing disk                  |
| $A$   | expected actual contact area    | $V$       | sliding speed                             |
| $C$   | specific heat                   | $T$       | temperature rise                          |
| $h$   | average heat flux               | $z$       | height of asperity                        |
| $E$   | Young's modulus                 | $\mu$     | coefficient of friction                   |
| $K$   | thermal conductivity            | $\rho$    | density of material                       |
| $L$   | Load on PCD specimen            | $\nu$     | Poisson's ratio                           |
| $L_1$ | average force on an asperity    | $\chi$    | thermal diffusivity                       |
| $N$   | number of asperities            | $\Phi(z)$ | distribution function of asperity heights |
| $P'$  | normal pressure on PCD specimen | $\eta$    | density of asperities                     |
| $P$   | expected applied pressure       | $\omega$  | speed of rotation                         |
| $R$   | PCD asperity radius             | $\sigma$  | standard deviation                        |

calculations would help determine whether the temperature rise is high enough to stimulate a chemical reaction.

## 2. Modelling

Greenwood–Williamson's statistical asperity model will be used to characterise the surface roughness of a PCD specimen. The result will then be used to estimate the contact area and total number of contact asperities under an applied polishing load. The heat generated will be taken as the product of the friction force and the relative sliding velocity between the PCD asperities and the metal disk surface. The Jaeger's moving heat source analysis will then be applied to determine the fractions of heat flux flowing into the PCD asperities and their counterpart at contact sliding in polishing and to give rise to the average temperature rise on the contact surface.

### 2.1. Statistical model of PCD surface roughness

During polishing, the contact between a PCD surface and the polishing disk is on a large number of asperities.

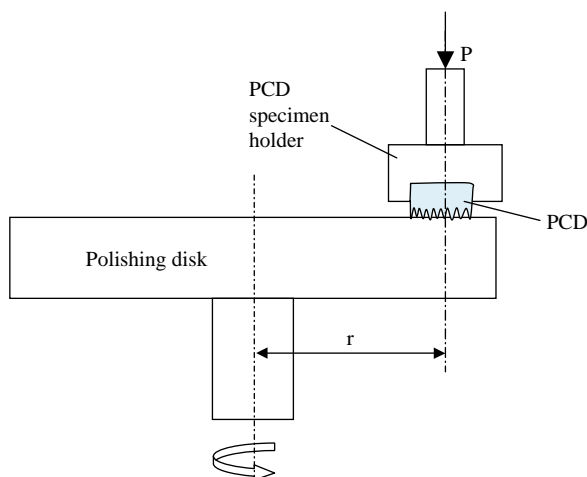


Fig. 1. Schematic illustration of dynamic friction polishing.

Random roughness of the PCD can be characterized by a statistical asperity model [17], which assumes: (i) that all asperities are spherical at their summits and have the same radius  $R$  and, (ii) that their heights vary randomly: the probability that a particular asperity has a height between  $z$  and  $z + dz$  above a reference plane, as illustrated in Fig. 2 will be  $\Phi(z) dz$ , where  $\Phi(z)$  is the height distribution of the PCD asperities. Fig. 2 shows the schematic of the contact surfaces. The behaviour of an individual asperity during contact can be found from the Hertzian equations [18]. It should be noted that the surface of the polishing metal disk is assumed to be smooth, since the metal is much softer than PCD so that the polishing forces acting through neighbouring disk asperities will influence each other, i.e. the individual contacts are not independent.

If the two surfaces come together until their reference planes are separated by a distance  $d$  (Fig. 2), then contact will occur at any asperity whose height was originally greater than  $d$  [17]. So, the probability of making contact at any given asperity of height  $z$  is

$$\text{prob}(z > d) = \int_d^{\infty} \Phi(z) dz$$

If the surface density of asperities  $\eta$  and the nominal contact area  $A'$  are known, then the total number of asperities will be  $N = \eta A'$ . Thus the expected number of

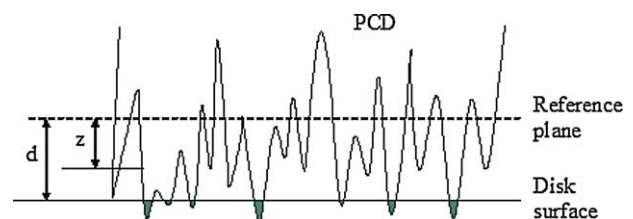


Fig. 2. Schematic of PCD asperities-disk contact in polishing (The load is supported by those shaded asperities whose heights are originally greater than the separation  $d$ ).

contacts will be

$$n = \eta A' \int_d^{\infty} \Phi(z) dz. \quad (1)$$

The expected total area of contact will be

$$A = \pi \eta A' R \int_d^{\infty} (z-d) \Phi(z) dz. \quad (2)$$

The expected total load is

$$L = \frac{4}{3} \eta A' E' R^{1/2} \int_d^{\infty} (z-d)^{3/2} \Phi(z) dz, \quad (3)$$

where

$$\frac{1}{E'} = \frac{1-\nu_1^2}{E_1} + \frac{1-\nu_2^2}{E_2} \quad (4)$$

in which  $E$  and  $\nu$  are Young's modulus and Poisson's ratio, and the subscripts 1 and 2 refer to the two contacting materials. The applied load  $L$  is carried by asperities in contact. The nominal pressure is  $P' = L/A'$ , and applied pressure is  $P = L/A$ , where  $A'$  is the nominal area of specimen and  $A$  is the expected contact area. Note that  $P \gg P'$  because  $A \ll A'$ , and that the actual contact area  $A$  is a strong function of surface roughness, but  $P$  is not. This suggests that  $P$  controls polishing via the actual contact area [19].

Thus, if the surface characteristic function of the PCD,  $\Phi(z)$ , and the applied load,  $L$ , are known, then the separation of the two surfaces can be calculated by using Eq. (3). The number of contacts  $n$  and the contact area  $A$  can then be obtained by using Eqs. (1) and (2).

## 2.2. Temperature rise

In order to estimate the temperature rise at contact between a PCD asperity and a polishing disk, the theory of a moving heat source and the method of energy partition at contacts developed by Jaeger [20] are used. The heat generated at the contact between a PCD asperity and the polishing disk is taken as the product of the friction force acting on the asperity and the relative sliding velocity  $V$  between the asperity and the disk. The average force  $L_1$  acting on the asperity is the total load divided by the number of contacts

$$L_1 = L/n = PA' / (\eta A') \int_d^{\infty} \Phi(z) dz = P/\eta \int_d^{\infty} \Phi(z) dz. \quad (5)$$

Since the summits of asperities are assumed to be spherical with radius  $R$ , and the contact is assumed to be Hertzian, the average contact radius of the asperity is

given by:

$$a = \sqrt{\frac{A}{\pi n}} = \sqrt{\frac{R \int_d^{\infty} (z-d) \Phi(z) dz}{\int_d^{\infty} \Phi(z) dz}}. \quad (6)$$

The average heat flux at the real area of contact due to the frictional heating can therefore be expressed as [20–22]

$$h = \frac{\mu L_1 V}{\pi a^2}, \quad (7)$$

where  $\mu$  is the coefficient of friction and  $V$  is the relative sliding velocity between the contacting bodies, which is determined from the relation  $V = r\omega$  (Fig. 1). For an individual asperity of PCD, the contact between the asperity and polishing disk is Hertzian, tangential friction force has a parabolic distribution, and the tangential frictional stress is given by [18]

$$q(x) = \frac{3\mu L_1}{2\pi a^3} (a^2 - x^2)^{1/2}.$$

Thus the heat flux generated due to the tangential friction force also has a parabolic distribution over the contact area.

The frictional heating of a PCD asperity can be modeled as a heat source moving over the surface of a semi-infinite polishing disk with velocity  $V$ , as the disk and PCD specimen are much bigger than the asperities. An analytical formulation for the temperature under a square or a band heat source moving over the surface of a semi-infinite solid was presented by Jaeger [20]. Later in 1994, Tian and Kennedy [21] derived an approximate solution for the interface temperature rise under a moving circular heat source for the entire range of Peclet numbers  $P_e$  which, representing the scale of the velocities in moving heat source, is defined as [21,22]

$$P_e = \frac{Va}{2\chi} = \frac{Va\rho C}{2K},$$

where  $\chi = K/(\rho C)$  is the thermal diffusivity,  $K$  is thermal conductivity,  $C$  is specific heat, and  $\rho$  is the density of the material exposed to the heat source. In this paper,  $P_e$  refers to the Peclet number of the polishing disk material.

The frictional heating of a PCD asperity can be modeled as a heat source moving over the surface of a semi-infinite polishing disk with velocity  $V$ . According to Tian and Kennedy [21], the average, steady-state surface temperature rise  $T$  over the area of contact due to a circular parabolic heat source  $h$  moving over a homogeneous semi-infinite solid with velocity  $V$  is

$$T = \frac{1.464ah}{K\sqrt{\pi(0.874 + P_e)}}. \quad (8)$$

For a stationary parabolic circular heat source  $h$ , the temperature rise is

$$T = \frac{9Q}{32RK} = \frac{9\pi ah}{32K} \quad (9)$$

According to Jaeger [20], when a steady state has been attained, it can be assumed that a fraction  $\alpha$  of the heat  $h$  per unit time per unit area generated over the area of contact passed on to the polishing disk and the remaining fraction  $(1 - \alpha)$  to the PCD asperity. The fraction  $\alpha$  can therefore be determined by the condition that at the contact interface, the average temperature on the disk surface equals that on the PCD surface, if there is no heat loss to the surroundings. Equating these temperature rises, given by Eqs. (8) and (9) for the asperity and the disk surfaces over the circularly shaped area of contact gives rise to

$$\frac{1.464ah\alpha}{K_d\sqrt{\pi(0.874 + P_e)}} = \frac{9\pi ah(1 - \alpha)}{32K_p} \quad (10)$$

The subscripts  $d$  and  $p$  refer to the disk and PCD asperity, respectively. From Eq. (10), the heat flux fraction  $\alpha$  going into the polishing disk is

$$\alpha = \frac{9\pi K_d\sqrt{\pi(0.874 + P_e)}}{46.848K_p + 9\pi K_d\sqrt{\pi(0.874 + P_e)}} \quad (11)$$

The contact temperature rise at the sliding interface is therefore:

$$T = \frac{13.176\pi ah}{46.848K_p + 9\pi K_d\sqrt{\pi(0.874 + P_e)}} \quad (12)$$

The above analysis gives an upper bound estimation because the heat loss into the surrounding has been neglected. Since the model calculates the average temperature rise on the asperity over the contact area, hot spot or flash temperatures, which could be significantly higher in polishing, cannot be estimated.

In the model developed above, when the applied load and the surface characteristics (including the function  $\Phi(z)$ , radius of asperity  $R$  and the asperity density  $\eta$ ) are known, the number of contacts  $n$  and the contact area  $A$  can be calculated by using Eqs. (1)–(3). Then from Eq. (7), the average heat flux  $h$  can be obtained after the average force  $L_1$  and the contact radius of asperity  $a$  are determined from Eqs. (5) and (6) respectively. Finally the average contact temperature rise can be calculated from Eq. (12).

### 3. Experimental measurement of surface topography

In order to calculate the expected number of contacts and total area of contact, the topographic parameters should be measured. These parameters include the radius of asperity summits, the surface density of asperities and the spread of asperity heights. For this purpose, the confocal microscope technique used by Zhang and Zarudi [23] was employed. With the confocal microscope, a series of pictures in focus on different layers can be obtained. Also these pictures can be compiled to an extended focus image; one such image

obtained in the present study which shows PCD asperities is depicted in Fig. 3(a). Then on a selected line, a surface roughness diagram can be acquired as shown in Fig. 3(b) to generate the surface roughness data.

By using the microscopy analysis software LEICA QWin, these extended focus images were analysed. From the results of asperity field analysis, the area of asperity, the number of asperities (count), the total area of analysed frame and the ratio of count to frame area were obtained. For the PCD compact used in the present experiment, the average asperity density  $\eta$  was found to be  $2.2 \times 10^5$  asperities/mm<sup>2</sup>. From an analysis of the asperity features, it was found that the mean equivalent diameter of asperities was 0.90  $\mu\text{m}$ , hence the average radius of the asperities was calculated to be 0.45  $\mu\text{m}$ .

By using an Excel statistical data analysis tool: *Histogram and Descriptive Statistics*, it was found that the asperity heights on the surface would approximately obey a Gaussian distribution,  $\Phi(z) = \frac{1}{\sigma\sqrt{2\pi}} e^{-z^2/2\sigma^2}$ , with an average height of 0 (which is the asperity height reading from the mean plane) and a standard deviation of 2.0  $\mu\text{m}$ . The standard deviation  $\sigma$  of the distribution is identical to

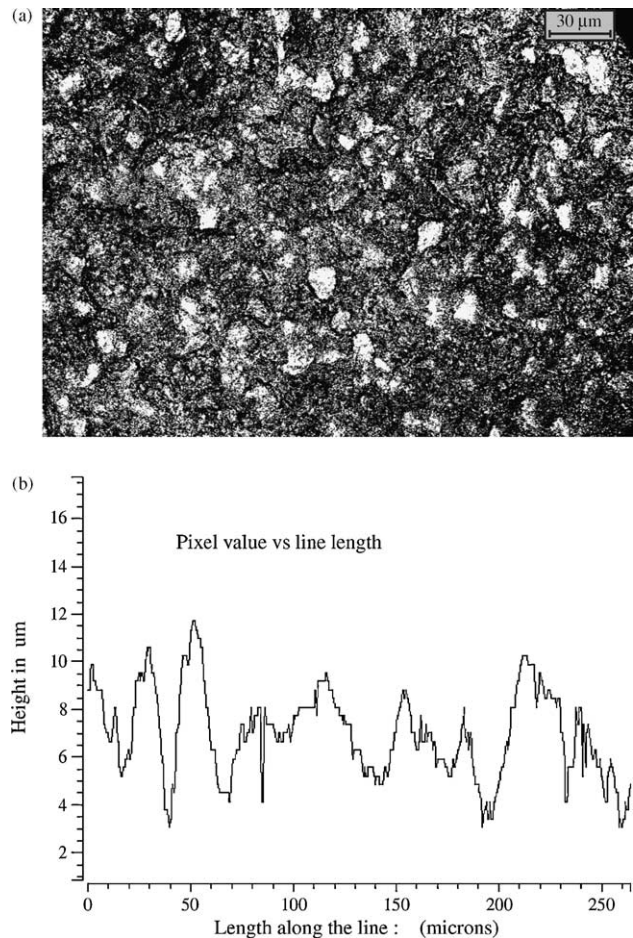


Fig. 3. The surface topography of a PCD specimen before polishing, generated by confocal microscopy. (a) The extended focus picture (b) Surface roughness diagram.

Table 1  
Properties of PCD and catalytic steel

|                          | Catalytic steel        | Polycrystalline diamond |
|--------------------------|------------------------|-------------------------|
| Young's modulus $E$      | 200 GPa                | 900 GPa                 |
| Poisson's ratio $\nu$    | 0.28                   | 0.10                    |
| Thermal conductivity $K$ | 16.3 W/m K             | 300 W/m K               |
| Density $\rho$           | 8000 kg/m <sup>3</sup> | 3520 kg/m <sup>3</sup>  |
| Specific heat $C$        | 500 J/kg K             | 470 J/kg K              |

the root mean square roughness value of the surface [24]. In the present work, the maximum asperity height was 5.0  $\mu\text{m}$  and hence this value was used instead of infinity for the integrations in Eqs. (1)–(3), (5) and (6).

It should be noted that the surface characteristics  $R$  and  $N$  of a randomly rough surface are not unique but depend on the resolution and the scan length of the roughness-measuring instrument [24]. Only the standard deviation  $\sigma$  can be approximately taken as scale-independent. Thus only the asperities which had a roughness of the same order of magnitude as that of the overall  $\sigma$  value can be counted.

## 4. Results and discussion

### 4.1. Predicted results

The contact temperature rise for the polishing of PCD using a steel disk, which acts catalytically with the diamond surface, has been estimated using the temperature model derived above. Table 1 gives the material properties of the PCD and the steel used for the calculations. It must be pointed out that the properties of PCD are strongly dependent on composition, particle size, and processing conditions [18]. For example, the thermal conductivity of a normal PCD can range from 250 to 920 W/m K [25–29]. For the present PCD, some of the data such as thermal conductivity, the Poisson's ratio and density were measured experimentally. The coefficient of friction between the disk and PCD asperity was taken to be 0.15 based on the measurement by Iwai et al [15]<sup>1</sup>. A MATLAB program was developed for calculating the temperature rise.

Figs. 4 and 5 show the variations of the calculated average contact temperature rise with the sliding velocity and nominal applied pressure. According to these figures, the higher values of  $P$  and  $V$  correspond to a higher heat flux  $h$  and higher temperature rise  $T$ . The temperature rise  $T$  is seen to increase with increasing  $P$  and  $V$ . The dependence of  $T$  on  $V$  appears to be linear for a fixed nominal pressure (Fig. 4). However, for a fixed sliding velocity  $V$ , the relation between  $T$  and  $P$  seems to follow by a power law (Fig. 5).

<sup>1</sup> The coefficient of dynamic friction was measured to be from 0.13 to 0.2 at pressures 17 and 27 MPa with a mean value of about 0.15.

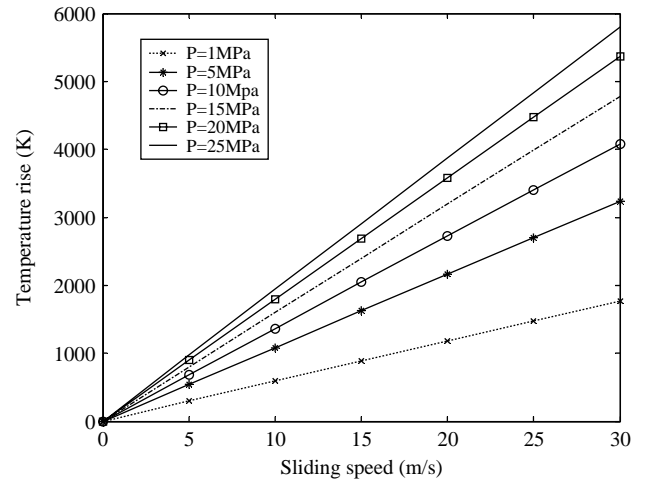


Fig. 4. Variation of average temperature rise with sliding speed at different nominal pressures.

It can also be seen that velocity has a greater influence on temperature rise  $T$  (indicated by a higher slope) than pressure.

From Eq. (12), it can be seen that the temperature rise is dependent on not only the sliding parameters ( $V$  and  $P$ ), but also the surface characteristics and properties of the two sliding materials, especially their thermal conductivities. Thus, we have also predicted the temperature rise for varying values of the PCD's thermal conductivity. The other data used for the calculation are given in Table 1. These predicted results are given in Fig. 6. As expected, higher values of PCD's thermal conductivity result in lower values of temperature rise at the interface. For example, when the thermal conductivity of PCD increases twice, the temperature rise drops to 50%.

The surface roughness of PCD also affects the temperature rise. Fig. 7 compares the temperature rise for different values of standard deviation  $\sigma = 1, 2$  and  $4 \mu\text{m}$ . In the calculations, the maximum height of the asperity was selected to be  $2.5\sigma$ , which is the appropriate value for

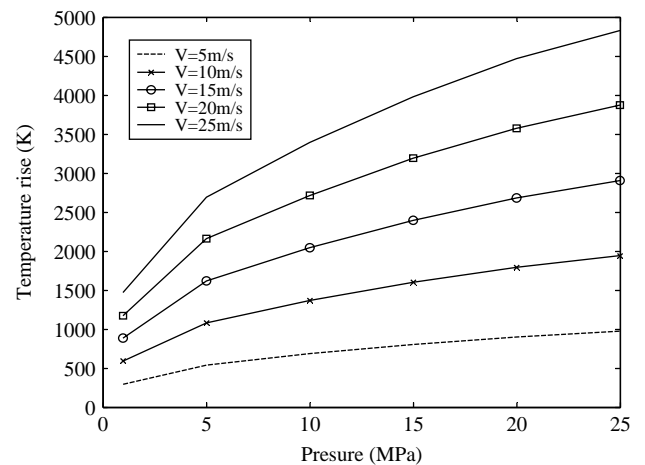


Fig. 5. Variation of average temperature rise with nominal pressure at different sliding speeds.

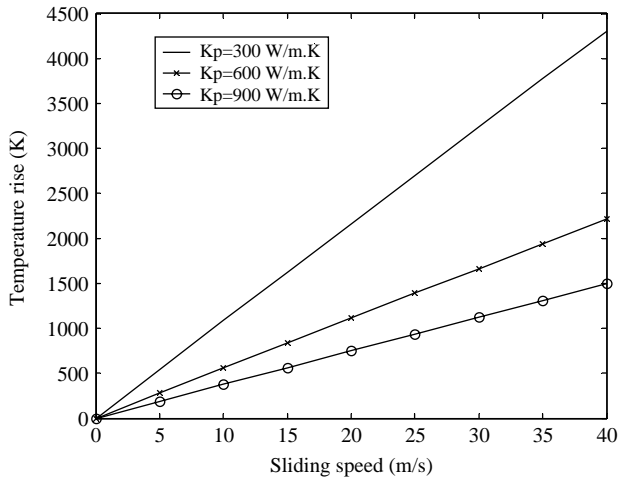


Fig. 6. Variation of temperature rise with sliding speed at different thermal conductivity of PCD at pressure 5 MPa.

the PCD used in the present work. The results given in Fig. 7 show that a higher surface roughness of PCD results in a higher temperature rise, since there are fewer asperities in contact under the same nominal pressure and hence a higher average load on contact asperities. This means that when polishing goes on, the polishing speed or pressure should be increased if one needs to maintain the same temperature rise for the sake of efficient polishing (neglecting the heat accumulation), because the surface roughness of a PCD specimen decreases during polishing.

In the above calculations, it was assumed that the material properties such as Young’s modulus  $E$  and thermal conductivity  $K$  would not vary with temperature. While the details on temperature-dependence of  $E$  and  $K$  for PCD could not be found, the information available seems to indicate that for both the catalytic steel and PCD,  $E$  decreases whereas  $K$  increases with the increase in temperature [25,30,31]. A decrease in  $E$  will cause an increase in pressure and hence an increase in the calculated

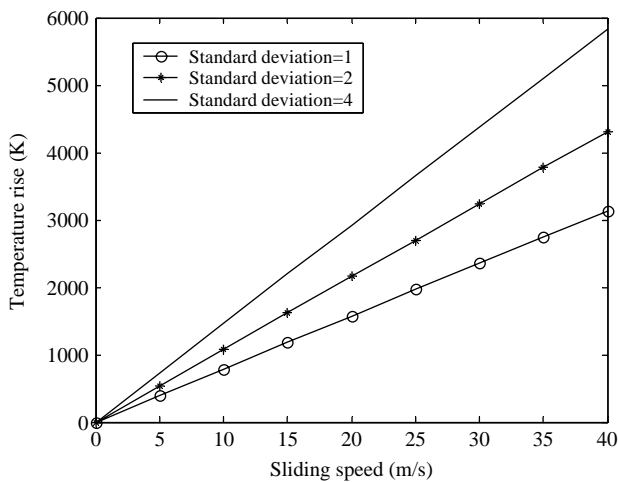


Fig. 7. Variation of temperature rise with sliding speed at different surface roughness at pressure 5 MPa.

temperature. On the other hand, an increase in  $K$  will lead to a decrease in the calculated temperature. Therefore, the variations of  $E$  and  $K$  with temperature may not have large influence on the calculated temperature rise due to the balancing of their opposing effects.

4.2. Comparison with experiments

A direct measurement of temperature rise at the polishing interface is almost impossible at the present, so is a direct quantitative comparison of the theoretical prediction with experimental ones. However, the following experimental observations support our theoretical estimations.

In one of the authors’ preliminary tests, the PCD surface topography was measured as described in Section 3. The polishing parameters were: sliding speed approximately 15 m/s and pressure 5 MPa. During polishing, the steel disk turned red, and lots of sparkles were observed. It was noted that due to the frictional heat, the steel disk surface melted and adhered to the PCD surface. Obviously, the temperature at the interface was raised above the melting point of steel (1421 °C). From our predicted results (shown in Fig. 4), the temperature rise for the above sliding speed and pressure is approximately 1600 °C. It is noteworthy that the interface temperature will not increase beyond the melting point of steel. In addition, as highlighted in Section 2.2, the developed model tends to overestimate the interface temperature, as it does not count for the heat loss to the surrounding environment. Therefore, the estimated temperature rise seems reasonable.

Iwai et al [15] reported that, at pressure 27 MPa and sliding speeds above 10.5 m/s, the polishing efficiency increased linearly with the increase in speed. However, at lower sliding speeds (i.e. those below 10.5 m/s), PCD could not be polished. The reason is that at low speeds, the temperature rise by the dynamic friction is not high enough for the fast chemical reaction of diamond to occur. In the present work, an attempt was made to predict the interface temperature using the described predictive method for the conditions used in [15]. The surface roughness and properties of PCD used in the above study which were kindly provided by Iwai [32] are given in Table 2. The properties of steel used in the calculations were the same as those given in Table 1. The average asperity radius  $R$  and asperity density  $N$  of PCD were assumed to be the same as those given in Section 3. For the conditions used by Iwai

Table 2  
Surface roughness and properties of the PCD used in [15,32]

|                                      |                        |
|--------------------------------------|------------------------|
| Young’s modulus $E$                  | 776 GPa                |
| Poisson’s ratio $\nu^a$              | 0.10                   |
| Thermal conductivity $K$             | 560 W/m K              |
| Density $\rho$                       | 4120 kg/m <sup>3</sup> |
| Surface roughness standard deviation | 0.63 $\mu$ m           |

<sup>a</sup> Since  $\nu$  is not given in [15,32], it is assumed to be the same as that of PCD used in the present study.

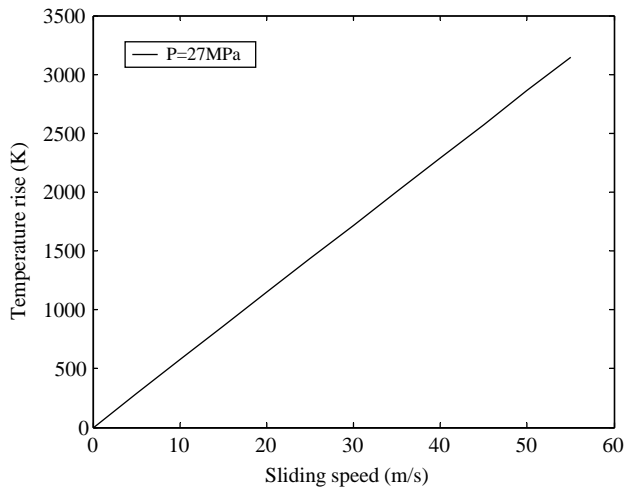


Fig. 8. Variation of temperature rise with sliding speed for the conditions used in [15,32].

et al, the predicted variation of temperature rise with sliding speed is shown in Fig. 8. It can be seen that, at sliding speed 10.5 m/s, the estimated temperature rise is approximately 650 °C. This value may be the minimum temperature rise required for the fast chemical reaction to occur at the PCD interface.

## 5. Conclusions

A theoretical model has been developed to estimate the average temperature rise in polishing PCD. The effects of PCD surface roughness, material properties of PCD, polishing velocity and polishing pressure on the surface temperature rise have been studied using the developed model. The model revealed that compared with changing the polishing load, increasing the sliding speed is a more effective way to raise the temperature at the interface for polishing efficiency. The experimental results published in the literature support the model's prediction.

## Acknowledgements

The authors wish to thank the Australian Research Council and Ringwood Superabrasives Pty. Ltd for their financial support for this research project. The authors appreciate that Dr M. Iwai provided further data on their experimental results which were not available in Ref. [15].

## References

[1] T.S. Sudarshan, *Polishing of diamond films- a review*, in *Surface Modification Technologies VIII*, T.S.S.M. Jeandin, Editor. 1995, The Institute of Materials.

- [2] A.P. Malshe, B.S. Park, W.D. Brown, A. Naseem, A review of techniques for polishing and planarizing chemically vapor-deposited (CVD) diamond films and substrates, *Diamond and Related Materials* 8 (7) (1999) 1198–1213.
- [3] B. Bhushan, V.V. Subramaniam, K. Gupta, Polishing of diamond films, *Diamond Films and Technology* 4 (2) (1994) 71–97.
- [4] S.E. Grillo, E. Field, The polishing of diamond, *J. Phys. D: Appl. Phys.* 30 (1997) 202–209.
- [5] F.M. van Bouwelen, Diamond polishing from different angles, *Diamond and Related Materials* 9 (3-6) (2000) 925–928.
- [6] C.D. Ollison, W.D. Brown, A.P. Malshe, H.A. Naseem, S. Ang, A comparison of mechanical lapping versus chemical-assisted mechanical polishing and planarization of chemical vapor deposited (CVD) diamond, *Diamond and Related Materials* 8 (6) (1999) 1083–1090.
- [7] J. Kuhnle, O. Weis, Mechanochemical superpolishing of diamond using NaNO<sub>3</sub> or KNO<sub>3</sub> as oxidizing agents, *Surface Science* 340 (1-2) (1995) 16–22.
- [8] M. Yoshikawa, Development and performance of a diamond film polishing apparatus with hot metals, *Proceedings of SPIE - The International Society for Optical Engineering* 1325 (1990) 210–221.
- [9] A.M. Zaitsev, Thermochemical polishing of CVD diamond films,, *Diamond and Related Materials* 7 (8) (1998) 1108–1117.
- [10] S. Jin, W. Zhu, E. Graebner, *Techniques for diamond thinning and polishing by diffusional reactions with metals*. in *Proceedings of the Applied Diamond Conference Applications of Diamond Films and Related Materials: Third International Conference (NIST SP 885)*. (1995) 1995.
- [11] R. Ramesham, F. Rose, Polishing of polycrystalline diamond by hot nickel surface,, *Thin Solid Films* 320 (2) (1998) 223–227.
- [12] H. Buchkremer-Hermanns, C. Long, H. Weiss, ECR plasma polishing of CVD diamond films, *Diamond and Related Materials* 5 (6-8) (1996) 845–849.
- [13] M.D. Shirk, P.A. Molian, P. Malshe, Ultrashort pulsed laser ablation of diamond, *Journal of laser applications* 10 (2) (1997) 64–70.
- [14] C. Vivensang, L. Ferlazzo-Manin, M.F. Ravet, G. Turban, F. Rousseaux, A. Gicquel, Surface smoothing of diamond membranes by reactive ion etching process, *Diamond and Related Materials* 5 (6-8) (1996) 840–844.
- [15] M. Iwai, T. Uematsu, K. Suzuki, N. Yasunaga, High efficiency polishing of PCD with rotating metal disc, *Proc. Of ISAAT2001(2001)* 231–238.
- [16] K. Suzuki, M. Iwai, T. Uematsu, N. Yasunaga, Material removal mechanism in dynamic friction polishing of diamond, *Key Engineering Materials Vols. 238-239 (2003)* 235–240.
- [17] J.A. Greenwood, B.P. Williamson, Contact of nominally flat surfaces, *Proc.R.Soc. London* 295 (1966) 300–319.
- [18] K.L. Johnson, *Contact mechanics*, Cambridge University Press, Cambridge, London.1985.
- [19] T.-K. Yu, C.C. Yu, M. Orłowski, A statistical Polishing Pad Model For Chemical-Mechanical Polishing., *IEEE IEDM: Washington DC*. p. (1993) 865–868.
- [20] J.C. Jaeger, Moving sources of heat and the temperature at sliding contacts, *Proceedings of the Royal Society of New South Wales* 76 (1942) 203–224.
- [21] X. Tian, E. Kennedy, Maximum and Average Flash Temperatures in Sliding Contacts, *AMSE Journal of Tribology* 116 (1994) 167–174.
- [22] V.H. Bulsara, Y. Ahn, S. Chandrasekar, N. Farris, *Polishing and lapping temperatures*. in *American Society of Mechanical Engineers (Paper) Proceedings of the ASME/STLE Joint Tribology Conference Oct 13-17. (1996)* 1996.
- [23] L. Zhang, I. Zarudi, An understanding of the chemical effect on the nano-wear deformation in mono-crystalline silicon components, *Wear* 225-229(Part 1) (1999) 669–677.
- [24] Y. Xie, A. Williams, The prediction of friction and wear when a soft surface slides against a harder rough surface, *Wear* 196 (1-2) (1996) 21–34.

- [25] B.J. Pope, M.D. Horton, H.T. Hall, S. DiVita, L.S. Bowman, N. Adaniya, Sintered diamond: its possible use as a high thermal conductivity semiconduction device substrate, Technical Progress Report - United States, Bureau of Mines (1975) 404–407.
- [26] J. Wilks and E. Wilks, Properties and applications of diamond, Butterworth Heinemann, 1994.
- [27] S. Jahanmir, M. Ramulu, and P. Koshy, eds. *Machining of ceramics and composites*. Marcel Dekker: New York, Basel. 1998.
- [28] S.A. Klimenko, Y.A. Mukovoz, G. Polonsky, Advance Ceramic Tools for Machining Application, Key Engineering Materials 114 (1996) 1–63.
- [29] J.E. Field, The Properties of Natural and Synthetic Diamonds, Academic Press, London. 1992.
- [30] J.D. Lord, Orkney, L.P., *Elevated Temperature Modulus Measurements using the Impulse Excitation Technique IET*, in *CMMT(MN) 049*. 2000, Crown: UK.
- [31] J.L. Lytton, J.A. Kren, K.T. Damber, D. Sherby, Apparatus for the determination of dynamic Young's modulus and internal friction in vacuum at temperatures from 25 °C to 1200 °C, BRIT, J. APPL. PHYS. 15 (1964) 1573–1583.
- [32] M. Iwai, *Personal e-mail communications*, 2005.